

Radiology-Pathology and Surgical Correlation in Astroblastoma

F. Sprenger, E.B. da Silva Jr, M.S. Cavalcanti, and B.C. de Almeida Teixeira

ABSTRACT

SUMMARY: Astroblastoma is a rare astrocytic glial neoplasm that affects mainly young girls, peaking between 10 and 30 years of age, with low- and high-grade manifestations. Imaging characteristics are well-described, but histopathologic and, more recently, molecular analysis is fundamental to establish the diagnosis, now based on *MNI* alterations. We describe a case with typical imaging and histologic features of an *MNI*-altered astroblastoma.

ABBREVIATIONS: 5-ALA = 5-aminolevulinic acid; AT/RT = atypical teratoid/rhabdoid tumor; GFAP = glial fibrillary acidic protein; K^{trans} = volume transfer constant

A 9-year-old girl with a previous diagnosis of high-functioning autism spectrum disorder presented with a 2-day history of headache, vomiting, and sleepiness. On the first day of symptoms, she was seen at a pediatric emergency department and discharged with anesthesia. Due to progressive worsening and unresponsiveness to medication, she was referred to a neurologic tertiary facility. The clinical examination showed a preserved consciousness level and no focal neurologic deficits or signs of meningeal irritation. Blood work had no relevant findings. MR imaging was performed to rule out intracranial pathology.

Imaging

MR imaging showed a large, well-circumscribed intra-axial heterogeneous mass in the right frontal lobe (Fig 1). The lesion had an eccentric, solid component isointense to gray matter on T1 and T2, with intense heterogeneous enhancement due to multiple, small, nonenhancing cysts within the solid portion, giving the lesion a bubbly appearance.

Larger cystic areas were observed on the periphery of the lesion with an intermediate signal on FLAIR and hyperintensity on T2. Foci of hypointensity on SWI and hyperintensity on the filtered phase were also seen and interpreted as punctate calcifications.

A slight perilesional FLAIR hyperintensity was present and attributed to vasogenic edema. There was small mass effect, with a little, leftward, midline shift and right lateral ventricle compression.

Advanced sequences demonstrated foci of intensely restricted diffusion ($ADC = 861 \times 10^{-6} \text{ mm}^2/\text{s}$), suggesting high cellularity, increased relative CBV ($1.8\times$), and increased volume transfer constant (K^{trans}) (0.170). MR spectroscopy showed increased Cho/Cr and Cho/NAA ratios (6.98 and 2.26, respectively), suggesting cellular membrane breakdown with neuronal depletion and a prominent lipid-lactate peak, inferring necrosis (Fig 2).

The above-mentioned findings suggested an aggressive primary supratentorial neoplasm, like high-grade astrocytoma, ependymoma, and embryonal tumor, mainly atypical teratoid/rhabdoid tumor (AT/RT). Despite its rarity and nonspecific manifestations, overlapping with characteristics of the above-mentioned tumors, astroblastoma was also considered, given the patient's age, the peripheral polymorph cysts, the solid enhancing portion with a bubbly appearance, and the well-circumscribed margins.

Neuraxis evaluation showed no additional lesions, and the patient underwent surgical resection 3 days after presentation at the tertiary center.

Operative Report

The patient was submitted to 5-aminolevulinic acid (5-ALA)-assisted microscopic near-total resection via frontal craniotomy. Perilesional thin-walled cysts were initially evacuated. The solid portion of the lesion was soft and heterogeneous, with an intense 5-ALA fluorescence and was resected with its capsule. The surgical cavity had faint 5-ALA positivity (Fig 3).

Intraoperative histopathologic examination showed a small-cell neoplasm with pseudorosettes, initially suggesting ependymoma.

Received September 7, 2022; accepted after revision February 17, 2023.

From the Department of Radiology (F.S., B.C.d.A.T.), Hospital de Clínicas da Universidade Federal do Paraná, Curitiba, Brazil; Department of Neurosurgery (E.B.d.S.), Instituto de Neurologia de Curitiba, Curitiba, Brazil; and Neopath Patologia Diagnóstica (M.S.C.), Curitiba, Brazil.

Please address correspondence to Flávia Sprenger, MD, Department of Radiology, Rua General Carneiro, 181, Curitiba, Paraná, Brazil, 80060-900; e-mail: flaviasprenger@gmail.com

<http://dx.doi.org/10.3174/ajnr.A7824>

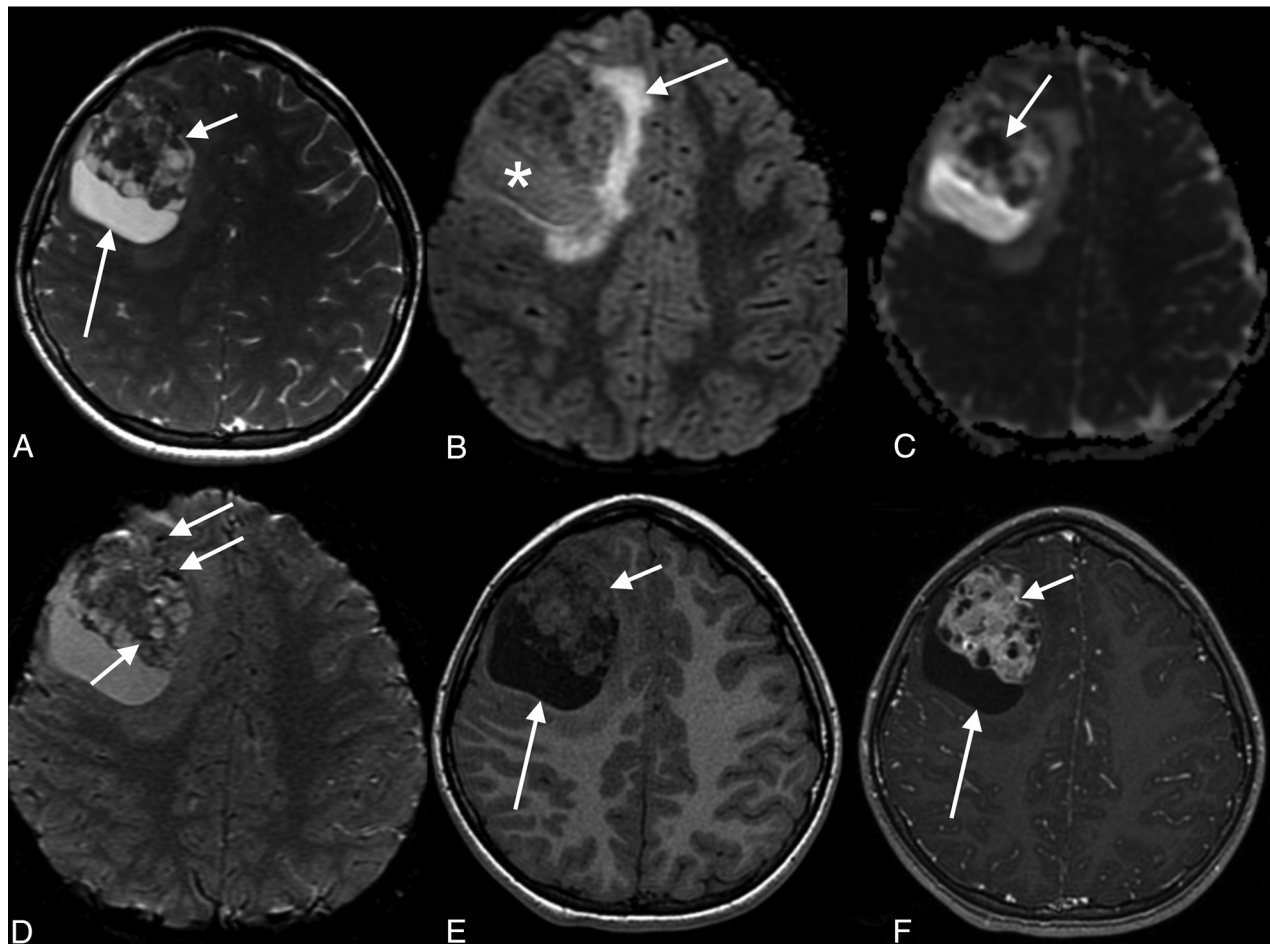


FIG 1. MR images and tumor characterization on multiple sequences. A, Axial T2 image shows the right frontal solid-cystic mass, with large peripheral cysts (*long arrow*) and an eccentric bubbly-appearing solid component (*short arrow*). B, Axial FLAIR demonstrates that the signal intensity of the content of the peripheral cyst is not suppressed (*asterisk*), as well as mild perilesional edema (*arrow*). C, ADC map shows foci of intensely restricted diffusion on the anterior and solid aspect of the lesion (*arrow*). D, Axial SWI demonstrates foci of marked hypointensity (*arrows*), corresponding to punctate calcifications according to the filtered phase signal (not shown). E, Axial T1 image demonstrates an isointense to gray matter heterogeneous solid portion (*short arrow*) with a hypointense large peripheral cyst (*long arrow*). F, Axial T1 postgadolinium image shows intense heterogeneous enhancement of the solid part, with multiple small permeating cysts, giving the tumor a bubbly aspect (*short arrow*). The large peripheral cysts show no enhancement (*long arrow*).

Pathology: Astroblastoma

Grossly, the tumor was fragmented and was tan and soft, with an identifiable cystic membrane.

Histopathologic examination showed solid sheets and pseudopapillae of rhabdoid cells oriented radially toward vessels, forming astroblastic pseudorosettes (Fig 5). Findings also included necrosis and easily recognizable mitoses (up to 4 mitoses/10 high power fields).

Immunohistochemistry was positive for glial fibrillary acidic protein (GFAP) antibody, epithelial membrane agent, and D2-40 (podoplanin), with a Ki-67 index of 25%. Integrase interactor 1 (*INI-1/SMARCB1*) expression was retained. The final diagnosis was astroblastoma. *MNI* profiling was not possible due to limited availability.

Pathologic differential diagnosis is challenging, especially with ependymomas, because they also present with perivascular pseudorosettes. Astroblastic pseudorosettes, however, have distinct columnar, tapered, or cuboid cell borders oriented radially around a hyalinized vessel. On the other hand, ependymal pseudorosettes

have unclear cell borders within a fibrillary perivascular area.¹ Supratentorial ependymomas also tend to have infiltrative margins, not seen in our case, and *RELA*-fused tumors show *LICAM* positivity on immunohistochemistry.

High-grade astrocytomas present as infiltrating astrocytic neoplasm with fibrillar glial processes, necrosis, and microvascular proliferation. Immunohistochemistry is positive for isocitrate dehydrogenase 1 (*IDH1*).² These morphologic differences ruled out this diagnosis in our case.

Angiocentric glioma, gemistocytic astrocytomas, and glioblastomas can also present with focal areas of perivascular pseudorosettes and their infiltrative characteristics. Therefore, astroblastoma diagnosis should be reserved for well-circumscribed gliomas in which the gliovascular characteristic is the main finding.³

AT/RT has variable patterns of histopathologic and immunostaining, consisting of rhabdoid cells, in addition to a small, blue, round cell component, and variable foci of mesenchymal or epithelial differentiation. Immunohistochemistry is usually positive for vimentin and epithelial membrane agent, and characteristically,

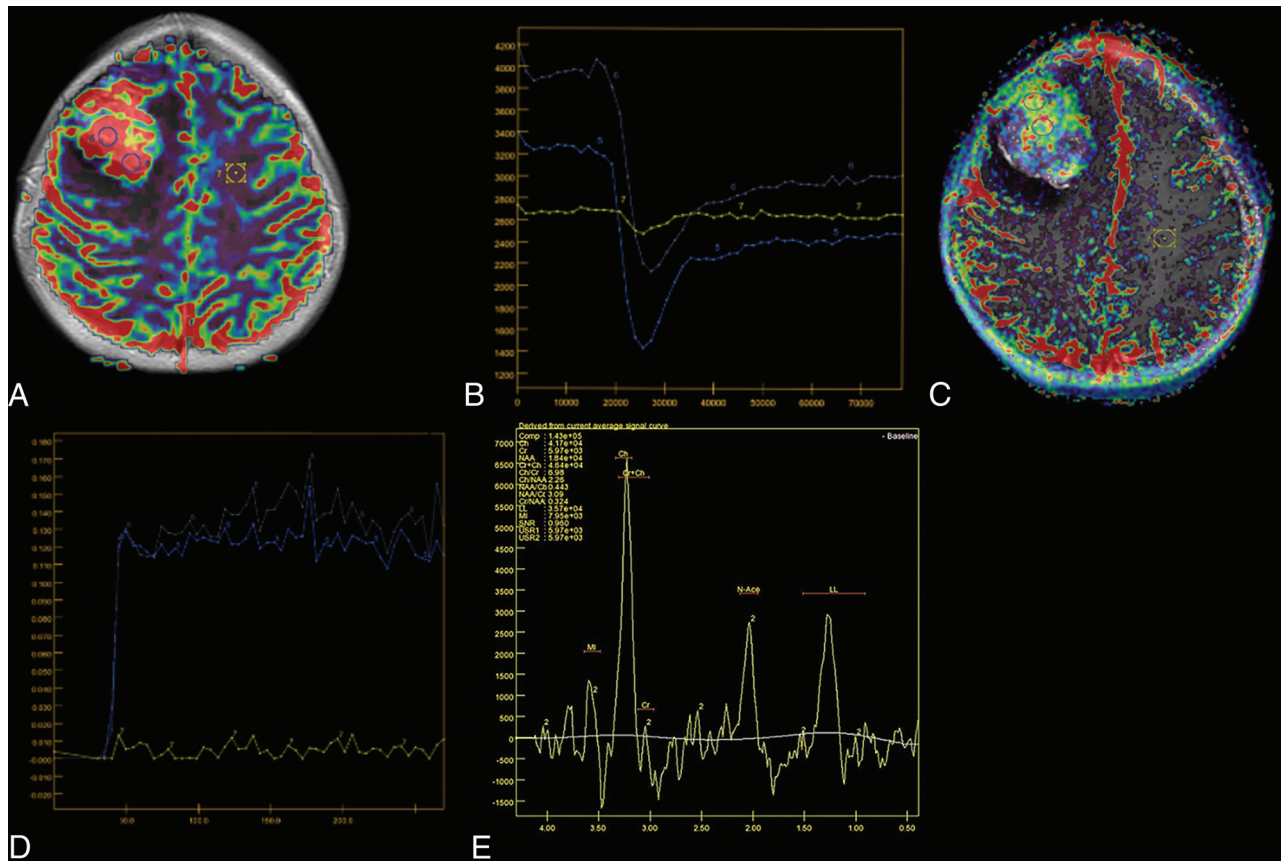


FIG 2. Advanced MR imaging features. *A* and *B*, Axial relative CBV map and curves, respectively, show intensely increased perfusion ($1.8\times$) within the solid part of the tumor, raising suspicion for a high-grade lesion. *C* and *D*, T1 perfusion K^{trans} map and curves, respectively, demonstrate intensely increased permeability and K^{trans} values in the enhancing portion of the lesion (0.170), suggesting increased capillary permeability. *E*, Proton spectroscopy shows an increased Cho peak, with increased Cho/Cr and Cho/NAA ratios, inferring cellular proliferation, as well as an increased lipid-lactate peak, suggesting anaerobiosis. LL indicates lipid lactate; USR1/2, Muon spin rotation; N-ace, N-acetylaspartate; MI, myoinositol.

there is a loss of either *INI-1/SMARCB1* or *SMARCA4*, the defining feature of this entity.⁴

DISCUSSION

Astroblastoma is a rare circumscribed astrocytic glial neoplasm, representing <3% of all gliomas, affecting mainly the cerebral hemispheres with a peak incidence between 10 and 30 years of age. Some series describe a higher prevalence in female patients.^{3,5,6} Its biologic behavior ranges from indolent to aggressive lesions, and a World Health Organization grade has not yet been attributed.¹

Historically, astroblastomas were initially described by Bailey and Cushing in 1924,⁷ but their histopathologic and molecular features overlapping with diffuse astrocytomas, pleomorphic xanthoastrocytomas, and ependymomas have led to decades of confusion. It has been described as a stage of glioma dedifferentiation, a fiber-producing astrocytoma, or rare tanyocytes or ependymal astrocyte neoplasm. The term itself is confusing because they are not notoriously astrocytic nor blastic. Only recently, assisted by molecular advances, their reliable diagnostic criteria have been established.^{3,5,6} Recent genetic profiling of high-grade neuroepithelial tumors revealed that many of the lesions with recurrent *MNI* mutations had histologic features of astroblastoma.⁸

The *MNI* gene, located in chromosome 22, is involved in meningioma and myeloid leukemia pathogenesis, and its rearrangements can be detected through DNA methylation. In addition to astroblastoma, many central nervous system primary tumors may express *MNI* alterations, like circumscribed and diffuse gliomas. Recently, this molecular signature has been attributed to the latter for more accurate diagnosis, but further research is needed to establish the ways these rearrangements act in astroblastoma and how it differs from manifestations in similar neuroepithelial tumors.⁹⁻¹²

Therefore, astroblastoma still shows molecular heterogeneity, with no exclusivity of *MNI* mutations in all cases, with most being classifiable within the *MNI* or *BRAF* DNA methylation groups.⁹ Despite minor heterogeneity, *MNI* alterations have become the defining feature of this condition in the 2021 World Health Organization CNS tumor classification, which is now called *MNI*-altered astroblastoma.¹⁰

Imaging usually reveals a supratentorial peripherally located solid-cystic mass with little or no vasogenic edema and rarely adjacent parenchyma infiltration (Figure 4). A bubbly aspect is frequently seen due to multiple cysts. Calcifications are seen in most cases, more commonly in a punctate pattern within the solid part. The solid component is usually isointense on T1 and T2/

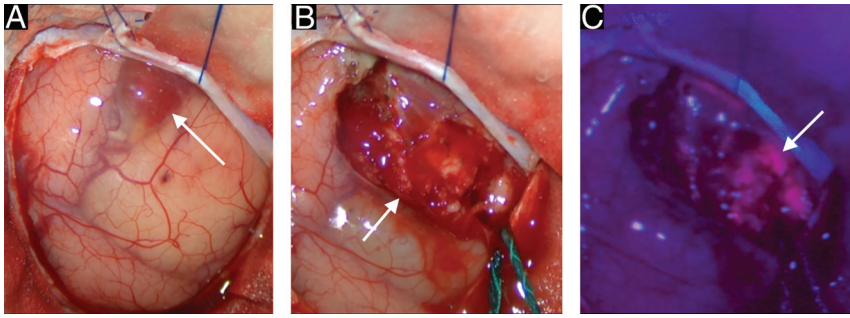


FIG 3. Intraoperative surgical microscope images. A, External view of the tumor demonstrates its peripheral cystic areas (arrow). B, Solid portion of the lesion after the cyst evacuation (arrow). C, The solid aspect of the tumor under blue light demonstrates its intense 5-ALA fluorescence (arrow).

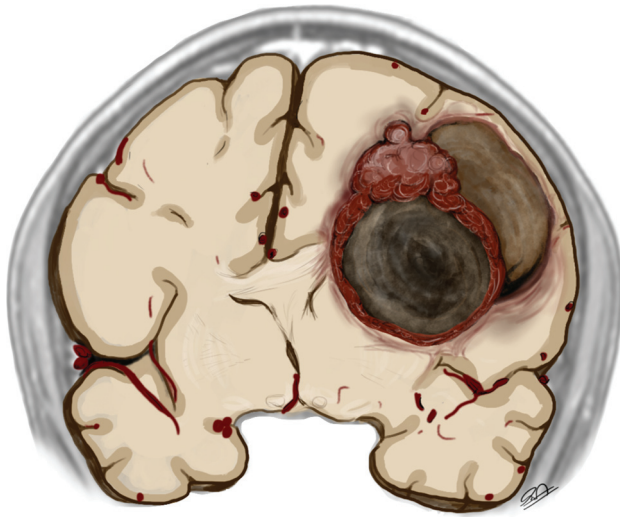


FIG 4. The schematic representation of astroblastoma consists of a hemispheric heterogeneous lesion with a lobulated solid and eccentric component and peripheral larger cysts. Note the faint perilesional edema, disproportional to the size of the lesion.

FLAIR, with a heterogeneous gadolinium enhancement and intermediate ADC values ranging from 1190 to $1250 \times 10^{-6} \text{ mm}^2/\text{s}$. Cystic areas are hyperintense on fluid-sensitive sequences and show facilitated diffusion. No MR imaging features can help differentiate indolent and malignant astroblastomas. Atypical presentations include solid masses with central necrosis and an irregularly rimmed cyst.^{3,6,13,14}

Imaging differential diagnosis includes supratentorial ependymomas, astrocytomas, and AT/RT.

YAP1 fusion-type ependymoma also presents as a heterogeneous mass with cystic areas. However, it is more prevalent among younger children, usually younger than 3 years of age. Due to its fibrillary components and infiltrative nature, perilesional edema and microinvasion are significantly more evident in ependymomas than in astroblastomas.^{6,15}

High-grade astrocytomas manifest less frequently in children but also have imaging features that overlap with astroblastoma because presentation may also demonstrate a heterogeneous supratentorial mass. Similar to ependymomas, mass effect and

perilesional infiltration are more striking in astrocytomas compared with astroblastomas.¹⁶

AT/RT may also present as large supratentorial heterogeneous masses, with a peak incidence in younger children around 3 years of age. Imaging demonstrates solid-cystic masses, with frequent hemorrhage and intensely restricted diffusion, in contrast to astroblastoma. Leptomeningeal dissemination is also frequent in AT/RT but not expected in astroblastoma.⁴

Macroscopically, astroblastomas present as well-circumscribed solid-cystic masses with a bubbly appearance secondary to cystic degeneration.

Microscopic features include elongated eosinophilic cells with GFAP-positive processes oriented radially from the cell body toward a usually hyalinized vessel, resembling ependymal perivascular pseudorosettes, but with a tapering or columnar aspect. Immunohistochemistry shows positivity for epithelial membrane agent and D2-40. GFAP, *OLIG2*, and S-100 are often positive to variable extents (Fig 5).³

Histologic features that indicate an aggressive biologic behavior include increased mitotic activity, palisading necrosis, high cellularity, vascular proliferation, and a high Ki-67 index. Higher Ki-67 indexes are also related to prognosis and survival rates, with a cutoff of 4%.¹

A primary histopathologic differential diagnosis includes high-grade astrocytomas, supratentorial ependymomas, atypical teratoid/rhabdoid tumors, and gemistocytic astrocytoma and these are better discussed in the previous session (See Pathology: Astroblastoma).

Treatment relies on gross surgical resection whenever possible. Low-grade lesions with satisfactory excision are usually followed up. Patients with incomplete resection or high-grade features in histology usually undergo adjuvant radiation and systemic chemotherapy with temozolomide.^{12,17}

Our patient had an excellent postoperative evolution, and 6-month control imaging shows no signs of recurrence. However, the multidisciplinary team opted for isolated adjuvant surgical cavity radiation due to faint 5-ALA surgical cavity positivity, necrosis, and mitotic activity. Systemic chemotherapy was not initiated.

Due to its rarity and imprecise imaging and histopathologic features, misdiagnosis is frequent. The ensemble of nonspecific features is the key. Astroblastoma should be remembered when this set of features is present, especially in a young female patient with a large, well-circumscribed hemispheric solid-cystic lesion.

Case Summary

- Astroblastoma is a rare intra-axial and hemispheric neoplasm typically present in adolescents and young adults.
- Imaging findings are not specific and include a heterogeneous mass with peripheral cysts and a solid bubbly-appearing component, overlapping with other tumors that affect children and young patients.

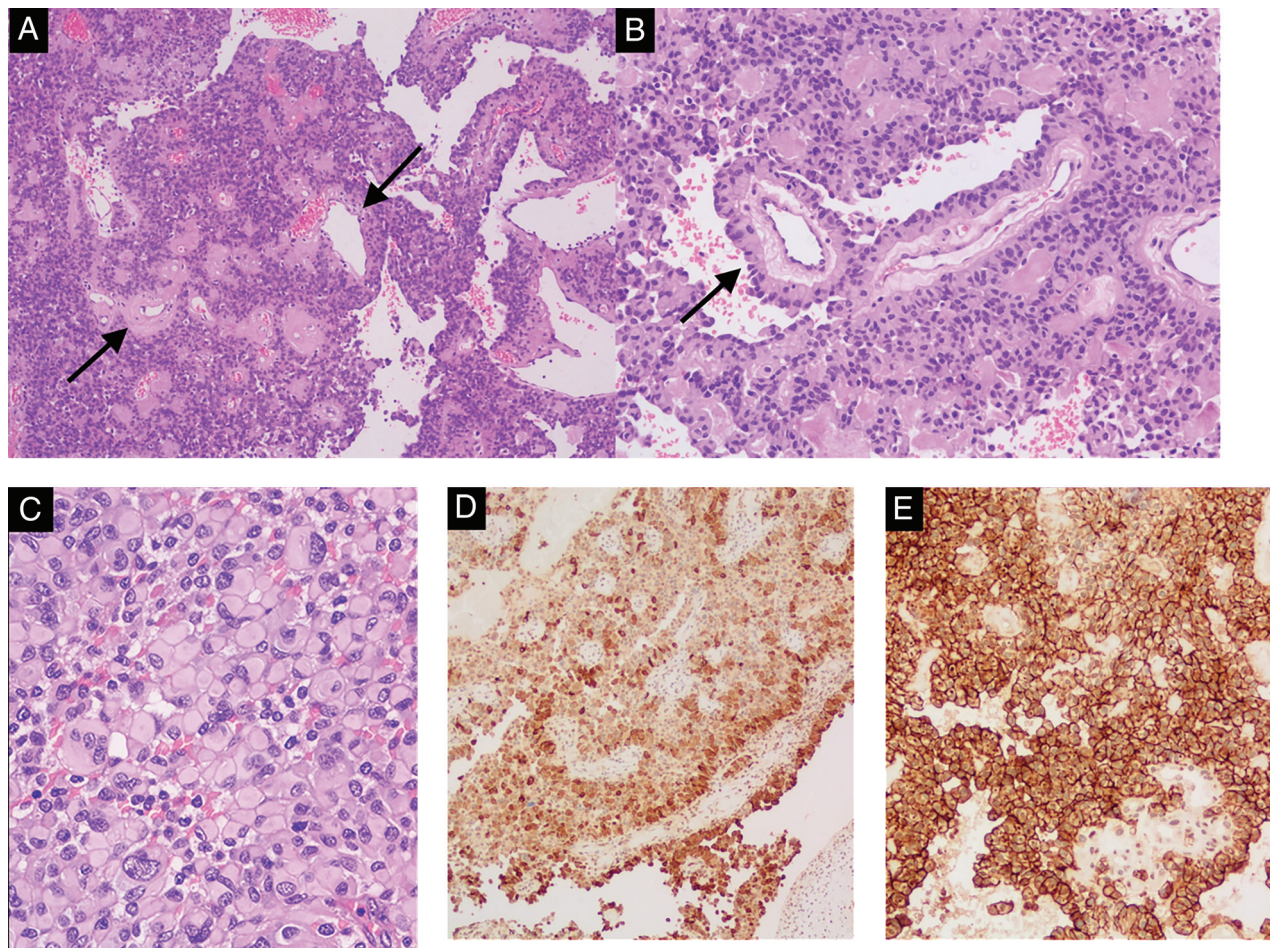


FIG 5. Pathologic findings of astroblastoma. *A*, The lesion was composed of solid sheets and pseudopapillae, with prominent hyalinized vessels (arrows), H&E, original magnification $\times 100$. *B*, Tumor cells have well-defined cytoplasmic borders, a columnar aspect radially arranged around the hyalinized blood vessels, forming astroblastic pseudorosettes (arrow), H&E, original magnification $\times 100$. *C*, Tumor shows rhabdoid features consisting of large cells with abundant eosinophilic cytoplasm and eccentric nuclei, H&E, original magnification $\times 100$. Tumor cells are diffusely positive for GFAP (*D*, immunohistochemistry, original magnification $\times 100$) and D2-40 (*E*, immunohistochemistry, original magnification $\times 200$).

- Pathologic differentiation from ependymoma can be challenging because both show perivascular rosettes. Subtle morphologic features can help differentiate astroblastic from ependymal pseudorosettes.
- Recently, *MN1* gene alterations have come to define this condition, which is now entitled *MN1*-altered astroblastoma.
- The main imaging differential diagnoses include high-grade astrocytomas, AT/RT tumors, and supratentorial ependymoma.
- Prognosis varies according to the presence of high-grade histologic findings, which also dictate adjuvant therapy.

Disclosure forms provided by the authors are available with the full text and PDF of this article at www.ajnr.org.

REFERENCES

1. Lehman NL, Hattab EM, Mobley BC, et al. Morphological and molecular features of astroblastoma, including BRAFV600E mutations, suggest an ontological relationship to other cortical-based gliomas of children and young adults. *Neuro Oncol* 2017;19:31–42 [CrossRef Medline](#)
2. Ichimura K, Narita Y, Hawkins CE. Diffusely infiltrating astrocytomas: pathology, molecular mechanisms and markers. *Acta Neuropathol* 2015;129:789–808 [CrossRef Medline](#)
3. Hammas N, Senhaji N, Alaoui Lamrani MY, et al. Astroblastoma: a rare and challenging tumor—a case report and review of the literature. *J Med Case Rep* 2018;12:102 [CrossRef Medline](#)
4. Zin F, Cotter JA, Haberler C, et al. Histopathological patterns in atypical teratoid/rhabdoid tumors are related to molecular subgroup. *Brain Pathol* 2021;31:12967 [CrossRef Medline](#)
5. Brat DJ, Hirose Y, Cohen KJ, et al. Astroblastoma: clinicopathologic features and chromosomal abnormalities defined by comparative genomic hybridization. *Brain Pathol* 2000;10:342–52 [CrossRef Medline](#)
6. Port JD, Brat DJ, Burger PC, et al. Astroblastoma: radiologic-pathologic correlation and distinction from ependymoma. *AJNR Am J Neuroradiol* 2002;23:243–47 [Medline](#)
7. Bailey P, Cushing H. *Classification of the Tumors of the Glioma Group*. Philadelphia, Pa: Lippincott;1926:83–84;133–136
8. Wood MD, Tihan T, Perry A, et al. Multimodal molecular analysis of astroblastoma enables reclassification of most cases into more specific molecular entities. *Brain Pathol* 2018;28:192–202 [CrossRef Medline](#)
9. Lehman NL, Usabalieva A, Lin T, et al. Genomic analysis demonstrates that histologically-defined astroblastomas are molecularly heterogeneous and that tumors with *MN1* rearrangement exhibit the most favorable prognosis. *Acta Neuropathol Commun* 2019;7:42 [CrossRef Medline](#)
10. Louis DN, Perry A, Wesseling P, et al. The 2021 WHO Classification of Tumors of the Central Nervous System: a summary. *Neuro Oncol* 2021;23:1231–51 [CrossRef Medline](#)

11. Saini M, Jha AN, Tangri R, et al. **MN1 overexpression with varying tumor grade is a promising predictor of survival of glioma patients.** *Hum Mol Genet* 2021;29:3532–45 [CrossRef Medline](#)
12. Petruzzellis G, Alessi I, Colafati GS, et al. **Role of DNA methylation profile in diagnosing astroblastoma: a case report and literature review.** *Front Genet* 2019;10:391 [CrossRef Medline](#)
13. Bell JW, Osborn AG, Salzman KL, et al. **Neuroradiologic characteristics of astroblastoma.** *Neuroradiology* 2007;49:203–09 [CrossRef Medline](#)
14. Kurokawa R, Baba A, Kurokawa M, et al. **Neuroimaging of astroblastomas: a case series and systematic review.** *J Neuroimaging* 2022;32:201–12 [CrossRef Medline](#)
15. Santosh V, Mangalore S, Aryan S, et al. **Imaging characteristics of supratentorial ependymomas: study on a large single institutional cohort with histopathological correlation.** *Asian J Neurosurg* 2015;10:276–81 [CrossRef Medline](#)
16. Okamoto K, Ito J, Takahashi N, et al. **MRI high-grade astrocytic tumors: early appearance and evolution.** *Neuroradiology* 2002;44:395–402 [CrossRef Medline](#)
17. Mallick S, Benson R, Venkatesulu B, et al. **Patterns of care and survival outcomes in patients with astroblastoma: an individual patient data analysis of 152 cases.** *Childs Nerv Syst* 2017;33:1295–302 [CrossRef Medline](#)